

Quantifying the nonlinear interaction in the nervous system based on phase-locked amplitude relationship

Yang, Yuan; Yao, Jun; Dewald, Julius ; van der Helm, Frans; Schouten, Alfred

DOI

[10.1109/TBME.2020.2967079](https://doi.org/10.1109/TBME.2020.2967079)

Publication date

2020

Document Version

Final published version

Published in

IEEE Transactions on Biomedical Engineering

Citation (APA)

Yang, Y., Yao, J., Dewald, J., van der Helm, F., & Schouten, A. (2020). Quantifying the nonlinear interaction in the nervous system based on phase-locked amplitude relationship. *IEEE Transactions on Biomedical Engineering*, 67(9), 2638-2645. <https://doi.org/10.1109/TBME.2020.2967079>

Important note

To cite this publication, please use the final published version (if applicable).
Please check the document version above.

Copyright

Other than for strictly personal use, it is not permitted to download, forward or distribute the text or part of it, without the consent of the author(s) and/or copyright holder(s), unless the work is under an open content license such as Creative Commons.

Takedown policy

Please contact us and provide details if you believe this document breaches copyrights.
We will remove access to the work immediately and investigate your claim.



Green Open Access added to TU Delft Institutional Repository

'You share, we take care!' - Taverne project

<https://www.openaccess.nl/en/you-share-we-take-care>

Otherwise as indicated in the copyright section: the publisher is the copyright holder of this work and the author uses the Dutch legislation to make this work public.

Quantifying the Nonlinear Interaction in the Nervous System Based on Phase-Locked Amplitude Relationship

Yuan Yang , Jun Yao, *Member, IEEE*, Julius P. A. Dewald, *Member, IEEE*, Frans C. T. van der Helm, and Alfred C. Schouten 

Abstract—Objective: This paper introduces the Cross-frequency Amplitude Transfer Function (CATF), a model-free method for quantifying nonlinear stimulus-response interaction based on phase-locked amplitude relationship. **Method:** The CATF estimates the amplitude transfer from input frequencies at stimulation signal to their harmonics/intermodulation at the response signal. We first verified the performance of CATF in simulation tests with systems containing a static nonlinear function and a linear dynamic, i.e., Hammerstein and Wiener systems. We then applied the CATF to investigate the second-order nonlinear amplitude transfer in the human proprioceptive system from the periphery to the cortex. **Result:** The simulation demonstrated that the CATF is a general method, which can well quantify nonlinear stimulus-response amplitude transfer for different orders of nonlinearity in Wiener or Hammerstein system configurations. Applied to the human proprioceptive system, we found a complicated nonlinear system behavior with substantial amplitude transfer from the periphery stimulation to cortical response signals in the alpha band. This complicated system behavior may be associated with the nonlinear behavior of the muscle spindle and the dynamic interaction in the thalamocortical radiation. **Conclusion:** This paper provides a new tool to identify nonlinear interaction in the nervous system. **Significance:** The

results provide novel insight of nonlinear dynamics in the human proprioceptive system.

Index Terms—Cross-frequency Interaction, Nonlinear System, EEG, Nervous System, Human Proprioceptive System, Frequency Domain Analysis.

I. INTRODUCTION

NERVOUS systems are highly nonlinear, showing harmonic (a positive integer multiple of the stimulation frequency, e.g., $3f_i$) and intermodulation (the sum or difference among multiple stimulation frequencies or their harmonics, e.g., $2f_i + 3f_j$) responses to periodic stimuli [1], [2]. For example, a recent study reported that over 80% of the cortical response to a periodic mechanical stimulus to the wrist joint is caused by nonlinear behavior of the somatosensory system [3]. Thus, assessing nonlinear relations between the stimulus and cortical response may improve our understanding of the communications in the nervous system and could lead to an increased insight of normal and pathological functions [4]–[6].

Several methods have been proposed to investigate nonlinear interactions in the nervous system, including time domain and frequency domain approaches [7]–[9]. A linear system is known to generate the response *only* in the same frequencies as the stimulus, i.e., the *iso-frequency* interaction between the stimulus and the response. Thus, in the frequency domain, the presence of nonlinearity can be detected by inspecting the harmonic and intermodulation of stimulation frequencies in the power spectral density (PSD) of the response. However, the PSD is computed on one single signal (either the stimulus or the response), so it cannot directly quantify the interaction between the stimulus and the response across different frequencies (i.e., stimulation frequencies vs. harmonics/intermodulations).

In terms of cross-frequency coupling measures, most existing methods for nervous systems focus on *phase* relation to quantify the nonlinear interaction between the stimulus and the response. Generalized phase synchrony measures, such as the *multi-spectral phase coherence* [10] and the *n:m phase synchronization index* [11], quantify the cross-frequency phase coupling independent of signal amplitude. To incorporate the effect of signal amplitude, high-order spectral coherence measures, such as *bicoherence* and *cross-spectral coherence*, were developed to assess nonlinearity in the nervous system [12]–[14]. However,

Manuscript received August 8, 2019; revised November 12, 2019 and January 3, 2020; accepted January 13, 2020. Date of publication January 16, 2020; date of current version August 20, 2020. This work was supported in part by the Dixon Translational Research Grants Initiative (PI: Yang) at Northwestern Medicine and Northwestern University Clinical and Translational Sciences Institute under Grants UL1TR001422 and NIH/NICHD 1R21HD099710 (PIs: Dewald, Yang), and in part by the European Research Council under the ERC Grant agreement 291339 (PI: van der Helm). (Corresponding author: Yuan Yang.)

Y. Yang is with the Department of Physical Therapy and Human Movement Sciences Feinberg School of Medicine, Northwestern University, Chicago, IL 60611 USA (e-mail: yuan.yang@northwestern.edu).

J. Yao is with the Department of Physical Therapy and Human Movement Sciences Feinberg School of Medicine, Northwestern University.

J. P. A. Dewald is with the Department of Physical Therapy and Human Movement Sciences Feinberg School of Medicine, Northwestern University, and with the McCormick school of Engineering, Northwestern University, and with the Department of Biomechanical Engineering, Delft University of Technology, and also with the MIRA Institute for Biomedical Technology and Technical Medicine, University of Twente.

F. C. T. van der Helm is with the Department of Biomechanical Engineering, Delft University of Technology, and also with the Department of Physical Therapy and Human Movement Sciences Feinberg School of Medicine, Northwestern University.

A. C. Schouten is with the Department of Biomechanical Engineering, Delft University of Technology, and also with the MIRA Institute for Biomedical Technology and Technical Medicine, University of Twente.

Digital Object Identifier 10.1109/TBME.2020.2967079

these measures only indicate the consistency of the stimulus-response coupling across trials rather than quantify the nonlinear amplitude transfer from the stimulus to the response.

Several studies used sophisticated nonlinear system identification approaches such as Volterra-Wiener Model [15] and NARMAX (nonlinear autoregressive moving average model with exogenous inputs) [16], [17] to investigate nonlinear transfer in biological systems [12], [18], [19]. Unlike the linear system identification approach (e.g., autoregressive with exogenous input) where the parameters can be relatively easily estimated, the parameter estimation in nonlinear system identification approaches requires a sophisticated procedure where an iterative method such as generalized least square algorithm is usually needed [16]. Furthermore, due to the complexity of the nervous system, the estimation of a complete model structure could be of considerably high dimensionality, and thus requiring a high computational cost. Therefore, to investigate amplitude transfer between stimuli and response in a complex nonlinear system, such as the nervous system, a model-free method can be appreciated.

To address these challenges, we propose a model-free approach for assessing the nonlinear amplitude transfer from the stimulus to the response in the nervous system, namely the **Cross-frequency Amplitude Transfer Function (CATF)**. CATF estimates the amplitude transfer from stimulation frequencies to their response harmonics/intermodulations. Different from generalized phase synchrony and nonlinear coherence methods, CATF assesses cross-frequency interaction in the nonlinear system based on amplitude transfer. Compared to model-based nonlinear system identification approaches, our method does not involve sophisticated parameter estimation and optimization procedures.

We first tested the proposed CATF method with model simulations using static nonlinear elements in series with linear dynamic systems (i.e., Hammerstein and Wiener systems). Then, we demonstrated the application of CATF to investigate the nonlinear amplitude transfer in the human proprioceptive system. Using both simulation and real physiological data, we demonstrated that CATF is suitable to probe an unknown (nonlinear) system and to pave the way for identifying a sophisticated system such as the human nervous system.

II. METHODS

The CATF estimates the phase-locked amplitude transfer from stimulation frequencies to their response harmonics/intermodulations in a nonlinear system. The CATF is developed based on the general nonlinear frequency mapping rule summarized in our previous study [14]. Thus, we first briefly introduce the concept of nonlinear frequency mapping and then propose the CATF. Model simulations are used to verify the proposed method. At the end of this section, we provide a description of the experimental dataset and demonstrate an application of our method to the human proprioceptive system.

We used a multi-sine signal, i.e., the sum of multiple sinusoids, as the stimulus signal for both simulations and experimental applications. A multi-sine signal can elicit a rich

class of nonlinear responses, including harmonics and intermodulations, and allows to validate our method [10], [14]. Furthermore, the multi-sine signal improves the SNR of the measured neural response [10], [15], [20].

A. Nonlinear Frequency Mapping

For an arbitrary nonlinear system, when the stimulus contains spectral components at multiple frequencies, such as a multi-sine signal, the harmonic and intermodulation responses can be generated. Let $X(f)$ and $Y(f)$ be the Fourier transforms of the stimulus signal $x(t)$ and the response signal $y(t)$. Assuming $X(f)$ contains N different frequencies f_1, f_2, \dots, f_N ($f_1 < f_2 < \dots < f_N$), the d -th order harmonic or intermodulation of the stimulation frequencies can be mathematically expressed as $f_{resp.} = \sum_{n=1}^N a_n f_n > 0$ ($\sum_{n=1}^N |a_n| = d$). A harmonic response is present when there is only one non-zero a_n ; and an intermodulation occurs when more than one a_n are non-zero.

The nonlinear mapping from the stimulus to the corresponding responses in the frequency domain for d -th order nonlinearity (e.g., $y = x^d$) can be summarized as:

$$Y(f_{resp.}) = H(f_1, f_2, \dots, f_N; a_1, a_2, \dots, a_N; f_{resp.})_d M \prod_{n=1}^N X^{a_n}(f_n) \quad (1)$$

$$\text{where } X^{a_n}(f_n) = \begin{cases} \underbrace{X(f_n)X(f_n) \cdots X(f_n)}_{a_n} & a_n > 0 \\ 1 & a_n = 0 \\ \underbrace{X^*(f_n)X^*(f_n) \cdots X^*(f_n)}_{|a_n|} & a_n < 0, \end{cases}$$

“*” indicates complex conjugate.

The M is the corresponding *multinomial coefficient*:

$$M = \frac{d!}{a_1! a_2! \cdots a_N!} \quad (2)$$

where “!” represents the factorial.

The $H(f_1, f_2, \dots, f_N; a_1, a_2, \dots, a_N; f_{resp.})_d$ is the d -th order *nonlinear mapping function* [14] for corresponding input frequencies f_1, f_2, \dots, f_N and their weights a_1, a_2, \dots, a_N to the response frequency $f_{resp.}$. The nonlinear mapping function is a *complex* value, which indicates amplitude scaling and phase change from the stimulus to the response.

B. CATF_B: Basic Estimator for Non-Overlapping Response Frequencies

Cross-frequency amplitude transfer function (CATF) is defined as the amplitude part (i.e., the magnitude) of the nonlinear mapping function, which reflects phase-lock amplitude transfer for the d -th order nonlinearity in the system. Noteworthy, when the stimulus contains multiple frequencies, different combinations of stimulation frequencies may result in the same response frequencies (e.g., $f_1 + f_2 = f_4 - f_3$); in this case, we consider $f_1 + f_2$ and $f_4 - f_3$ as overlapping frequencies in the response signal.

We first discuss the case where there is no overlap of response frequencies, then the d -th order CATF can be computed by:

$$CATF_B(f_1, f_2, \dots, f_N; a_1, a_2, \dots, a_N; f_{resp.})_d = \frac{|S_{xy}(f_1, f_2, \dots, f_N; a_1, a_2, \dots, a_N; f_{resp.})|}{M \prod_{n=1}^N S_{xx}^{[a_n]}(f_n)} \quad (3)$$

The $S_{xy}(f_1, f_2, \dots, f_N; a_1, a_2, \dots, a_N; f_{resp.})$ is the integer multiplication cross-spectrum [14]:

$$S_{xy}(f_1, f_2, \dots, f_N; a_1, a_2, \dots, a_N; f_{resp.}) = \langle \prod_{n=1}^N X^{a_n}(f_n) Y^*(f_{resp.}) \rangle \quad (4)$$

The $S_{xx}^{[a_n]}(f_n)$ is the high-order auto-spectra [14]:

$$S_{xx}^{[a_n]}(f_n) = \langle X^{[a_n]}(f_n) (X^{[a_n]}(f_n))^* \rangle \quad (5)$$

where $\langle \cdot \rangle$ represents the averaging over segments. The averaging is needed to reduce the noise.

When $d = 1$, Eq. (3) degrades to the *linear* case:

$$CATF_B(f) = \frac{|S_{xy}(f)|}{S_{xx}(f)} \quad (6)$$

Thus, the first-order CATF is identical to the gain (amplitude part) in the linear transfer function.

C. CATF: Estimator for Overlapping Response Frequencies

When combinations of stimulation frequencies can lead to overlapping response frequencies (i.e., $= \sum_{n=1}^N a'_n f_n$, $a_n \neq a'_n$), then $Y(f_{resp.})$ contains not only the response for the stimulation frequency combination with the weights a_1, a_2, \dots, a_R but also for that with a'_1, a'_2, \dots, a'_R . If the response generated by the combination of a_1, a_2, \dots, a_R is correlated with that generated by the combination of a'_1, a'_2, \dots, a'_R , then the estimator $CATF_B$ needs a correction.

Let $\gamma(f_1, f_2, \dots, f_N; a_1, a_2, \dots, a_N; f_{resp.})_d$ denotes the ratio between the basic estimator ($CATF_B$) and the truth value ($CATF_{TH}$), i.e., $\gamma = CATF_B / CATF_{TH}$. Then the Eq. (3) can be adapted to get the corrected CATF:

$$CATF(f_1, f_2, \dots, f_N; a_1, a_2, \dots, a_N; f_{resp.})_d = \frac{|S_{xy}(f_1, f_2, \dots, f_N; a_1, a_2, \dots, a_N; f_{resp.})|}{\gamma(f_1, f_2, \dots, f_N; a_1, a_2, \dots, a_N; f_{resp.})_d M \prod_{n=1}^N S_{xx}^{[a_n]}(f_n)} \quad (7)$$

For each overlapping frequency, the output response is the vector sum of the responses generated by different combinations based on the parallelogram law. While the cross-spectrum $S_{xy}(f_1, f_2, \dots, f_N; a_1, a_2, \dots, a_N; f_{resp.})$ projects the response at $f_{resp.}$ to a stimulus combination $(f_1, f_2, \dots, f_N; a_1, a_2, \dots, a_N)$ based on orthogonal decomposition. Thus, γ is the ratio between orthogonal decomposition and parallelogram decomposition. When the stimulus is fixed, the ratio γ is identical for all systems with the same order of nonlinearity. If the given system is $y = x^d$,

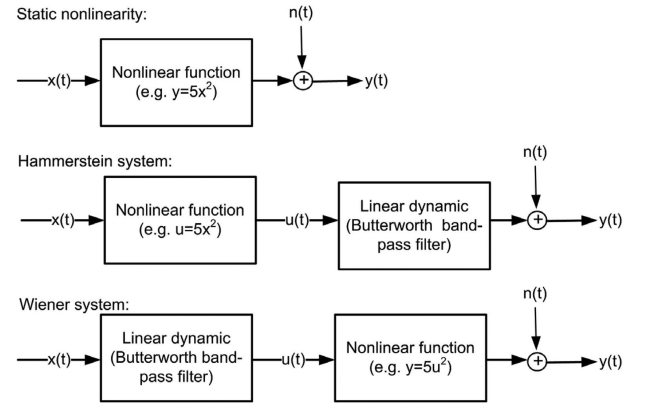


Fig. 1. Scheme of the three types of nonlinear systems used in the simulations.

then $CATF_{TH} = 1$ for all frequency combinations at d -th order nonlinearity and we have $\gamma = CATF_B$. Therefore, for a given stimulus and an unknown system (black box), we can first estimate $\gamma(f_1, f_2, \dots, f_N; a_1, a_2, \dots, a_N; f_{resp.})_d$ from the same order power function $y = x^d$ under a noise-free case using Eq. (3) (i.e., the basic estimator), and then apply Eq. (7) to the unknown system to get the (corrected) CATF for that order nonlinearity.

D. Model Simulations

We verified the performance of the CATF with static nonlinear functions and with Hammerstein and Wiener systems (see Fig. 1). We used the power function ($y = x^d$) as a static nonlinear function. According to Friston's review [21], most nonlinear interactions in neural systems can be approximated by the Volterra Series, which are polynomial series containing different orders of the monomial power function. Compared to other nonlinear functions, the advantage of the power function is that the generated harmonic and intermodulation responses to the stimulus are in the same order as the power (d) [10].

1) Static vs. Dynamic System: Without loss of generality, the CATF was first tested with the second-order (i.e., $y = 5x^2$) and third-order power functions (i.e., $y = 5x^3$) (see Fig. 1). We set the same scale (i.e., 5) for different systems for comparing the performance of CATF. Additionally, we also used Hammerstein and Wiener configurations (see Fig. 1) to test the CATF in dynamic systems, where the system dynamics are represented by a 5-th order Butterworth 8–35 Hz band-pass filter. For all tests, white noises were added to the output signals with the signal-to-noise-ratio (SNR) of -10 dB to represent the measurement noise.

2) No-Overlap vs. Overlap of Response Frequencies: The systems were firstly stimulated with a multi-sine signal (period: 1 s, 600 periods in total, sampling rate 2048 Hz) consisting of three sinusoids of 7, 13 and 29 Hz with randomly chosen phases. These three frequencies were chosen to avoid any overlap of the second-order and third-order harmonic and intermodulation frequencies, so the origins of the output frequency components can be easily visualized [10]. Additionally, we used another multi-sine signal consisting of 7, 13, 17 Hz

(other parameters are the same as the previous multi-sine signal) to demonstrate how the overlap of response frequencies affected the results using both basic (Eq. (3)) and corrected (Eq. (7)) estimators. These three stimulation frequencies can generate overlapping response frequencies at the third-order nonlinearity (and not at the second-order):

- **3 Hz:** $7 + 13 - 17$ (intermodulation of 7, 13 and 17 Hz), and $17 - 7 \times 2$ (intermodulation of 7 and 17 Hz),
- **21 Hz:** 7×3 (3rd order harmonic of 7 Hz), and $17 \times 2 - 13$ (intermodulation of 13 and 17 Hz),
- **27 Hz:** $7 \times 2 + 13$ (intermodulation of 7 and 13 Hz), and $17 \times 2 - 7$ (intermodulation of 7 and 17 Hz).

Thus, the results are only presented for the third-order power function in this test.

3) Evaluation: With the second-order nonlinear model simulations, we expect to have CATF in second-order harmonics and intermodulations. Similarly, we should have CATF in third-order harmonics and intermodulations for third-order nonlinear simulations. The CATF values should match the pre-set amplitude transfer in the simulation.

To evaluate the performance of the CATF, the amplitudes of the response frequency components $|\bar{Y}|$ at the frequency $f_{resp.}$ according to $f_1, f_2, \dots, f_N; a_1, a_2, \dots, a_N$ were reconstructed using the CATF:

$$\begin{aligned} |\bar{Y}(f_{resp.})| &= CATF(f_1, f_2, \dots, f_N; a_1, a_2, \dots, a_N; f_{resp.})_d \\ &\cdot M \left| \prod_{n=1}^N X^{a_n}(f_n) \right| \end{aligned} \quad (8)$$

and then were compared with the theoretical response component $|Y_{TH}(f_{resp.})|$ using normalized root-squared-mean-error (NRSME):

$$\begin{aligned} NRSME &= \sqrt{\frac{1}{N} \sum \left(\frac{|\bar{Y}(f_{resp.})| - |Y_{TH}(f_{resp.})|}{|Y_{TH}(f_{resp.})|} \right)^2} \times 100\% \end{aligned} \quad (9)$$

If there is an overlap of response frequencies, then $|Y_{TH}(f_{resp.})| = |Y(f_{resp.})| \cdot I\gamma(f_1, f_2, \dots, f_N; a_1, a_2, \dots, a_N; f_{resp.})_d$ and $|Y(f_{resp.})|$ is the amplitude of response at frequency $f_{resp.}$ measured from a noise-free simulation.

E. Application to the Human Proprioceptive System

We applied the CATF to investigate the nonlinear amplitude transfer in the human proprioceptive system. As shown previously [3], a large amount of the EEG (>80%) in response to the wrist perturbation is present in the non-excited harmonic and intermodulation frequencies. Our previous study provided us with a method to quantify the phase relationship between the perturbation and EEG [10]. This nonlinear phase transfer in the neural encoding of the external input is likely related to the time delay between the neural response and the stimulus [10]. Here, we investigate the nonlinear amplitude transfer, which is likely related to the scaling and filtering effect in the neural system [22].

The experimental datasets were recorded from seven healthy subjects (ages: 25 ± 2 , one woman) who performed 1 Nm isotonic flexion torque with the right wrist while a multi-sine position (angular) perturbation was applied. All participants signed informed consent and received financial compensation for their time. The experimental procedure was approved by the Human Research Ethics Committee of the Delft University of Technology. The multi-sine signal contained nine sinusoids with frequencies of 5, 7, 9, 11, 13, 16, 17, 23, 29 Hz and randomly chosen phases. Previous studies have indicated the importance of the second-order nonlinearity in the human proprioceptive system [3], [23], [24]. The designed multi-sine signal allows generation of nonlinear cortical response in different EEG frequency bands, including alpha (10–15 Hz), beta (15–30 Hz) and gamma bands (>30 Hz), which allows to check whether the amplitude transfer in the human proprioceptive system is mediated by the dynamics of any specific brain rhythms. The period of the multisine signal was 1 s and the peak-to-peak value was 0.06 radians. We kept the same velocity per frequency, since the proprioceptive sensor (i.e., muscle spindles) are most sensitive to velocity [24], [25].

During the experiment, subjects sat next to a wrist manipulator (WM), which is an actuated rotating device with a single degree of freedom to exert flexion and extension perturbations to the wrist joint (Wristalyzer, Moog Inc., The Netherlands). The right lower arm of subjects was strapped in the armrest while the right hand closely touched the handle of the WM (fixed with velcro). Subjects were instructed to relax their fingers and only use the wrist to perform the task. Wrist torque was measured by a force transducer equipped within the WM. To provide visual feedback of the torque, the signal was filtered online with a 1-Hz low-pass filter.

The experiment contained 40 trials. The trial started with a 1.5–2 s random period before the visual cue was shown. Subjects sat comfortably without any body movement during this period. After this period, subjects were visually guided to apply the 1 Nm isotonic flexion torque. When a steady force (1 ± 0.1 Nm) was generated for 2–3 s, the multi-sine perturbation started with a 1 s fade-in period and followed by a perturbed period of 30 s. The perturbation ended with a 1 s fade-out period. A random period of 8–10 s was set between the end of the trial and next trial; after a block of 10 trials, the subjects were given a break of a few minutes. The subjects were instructed to relax their forearm between trials to avoid possible muscle fatigue.

EEG was recorded using a 128-channel cap (5/10 systems, WaveGuard, ANT Neuro, Germany) with Ag/AgCl electrodes, using a common average reference. The EEG, perturbation, and torque signals were digitalized at 2048 Hz using a Refa amplifier (Twente Medical Systems International B.V., the Netherlands) and stored for offline analysis. We only used the data recorded during the 30-s perturbation period in each trial for analysis. All data were segmented into non-overlapping 1-s segments according to the period of perturbation signal, giving a frequency resolution of 1 Hz. This frequency resolution allows for detecting the harmonic and intermodulation responses, which are integer combinations of the three input frequencies (7, 13 and 17 Hz). Segments contaminated by artifacts in the EEG (e.g., blinking, eye movements and muscle artifacts) were removed by visual

inspection of the time series and power spectra of the EEG signals. The artifacts due to eye blinking and movement are typically shown in the electrodes over the frontal lobe, with a large amplitude ($>25 \mu\text{V}$) triangular (eye blink) or rectangle-shaped (eye movement or rotation) waveforms. Muscle artifacts are recognized by large power at high-frequency components ($>40 \text{ Hz}$), which is typically not present in normal EEG signal. During sensorimotor tasks, a normal EEG signal shows a spectrum decaying with frequency with peaks in the alpha and beta bands (between 10–30 Hz). After artifact removal, between 1002 and 1148 segments were included per subject. This amount of segments has been proven to be sufficient for a reliable nonlinear analysis in EEG [26]. The EEG data were detrended. All data were transformed to the frequency domain.

The human sensorimotor system is a closed-loop control system that include multiple neural circuits. In this study, we treated the whole system from the wrist to the brain as a “black” box. The perturbation signal is applied outside the physiological system and serves as an external input. Thus, the relationship between the perturbation and EEG represents uni-directional causality: the EEG response is evoked by the applied perturbation, and has no influence to the perturbation [25]. We performed CATF analysis at channel C3 to investigate the cross-frequency amplitude transfer from the perturbation to EEG activity at the sensorimotor cortex. We choose to use electrode C3 as C3 is around the sensorimotor area at the contralateral hemisphere to the stimulation of right wrist. Furthermore, the location of C3 is available in various EEG caps including basic and extended 10–20, 5–10 systems, from 16 channels to 256 channels. We focused on the second-order nonlinearity, whose importance has been indicated previously by showing stronger stimulus-response coupling than other orders [3], [10]. To confirm the dominance of the second-order nonlinearity in the EEG response, we also computed the FFT amplitude spectrum of the EEG component phase-locked to the 1-s perturbation signal, which was obtained by averaging the EEG over segments before computing its amplitude spectrum [3]. The results are presented as the spectrum of the EEG frequency, i.e., the response frequency, to check whether the amplitude transfer in the proprioceptive system is mediated by the dynamics of specific brain rhythms, such as alpha (10–15 Hz), beta (15–30 Hz) and gamma bands ($>30 \text{ Hz}$). Considering the individual difference, the CATF was normalized by the maximum value of CATF for each subject to get the spectra bounded by 0 and 1 for computing the grant averaging CATF over all subjects. We are mainly interested in how CATF varies with the EEG frequencies. Thus, if there is more than one stimulus frequency combination for an EEG response frequency, i.e., overlapping frequency mapping, then the mean CATF value was shown for that response frequency in the figures.

III. RESULTS

A. Simulations

All results are presented as the spectrum of response frequency. Fig. 2 shows the amplitude spectra of the nonlinear responses and the results of CATF for the second and third order power functions. The amplitudes of output components differ

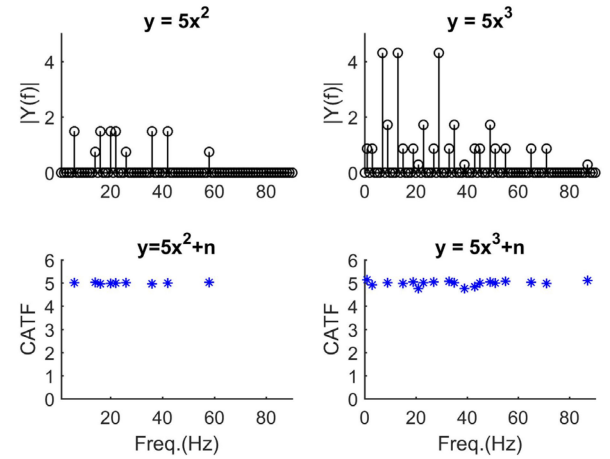


Fig. 2. Amplitude spectra of the nonlinear responses (noise-free case) and the results of CATF (SNR = -10 dB) for the second and third order power functions with the multisine stimulus of 7 13 29 Hz.

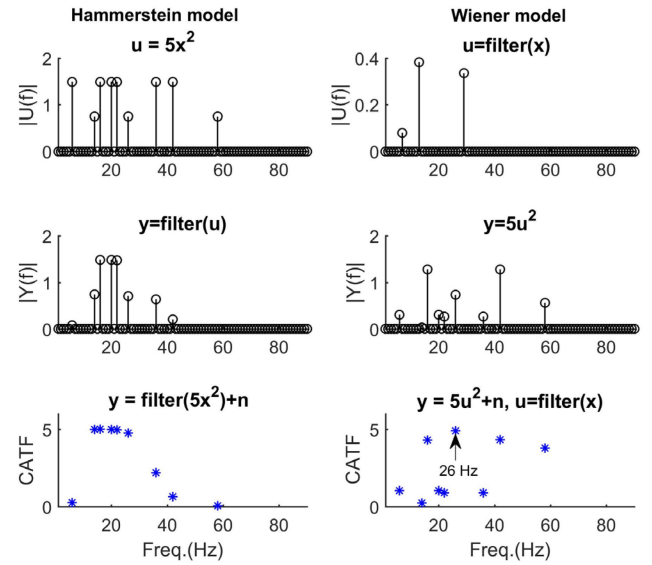


Fig. 3. Results for the Hammerstein and Wiener models for the multisine stimulus of 7 13 29 Hz. Upper row: amplitude spectra of signals $u(t)$. Middle row: amplitude spectra of signal $y(t)$ (noise free cases). Bottom row: the results of CATF (SNR = -10 dB).

between the harmonic and intermodulation responses for both second and third-order power functions. Thus, the amplitude transfer in a nonlinear system cannot be directly estimated from the amplitude spectra of the responses. Using CATF, the amplitude transfer can be well estimated, showing the CATF value around the pre-set theoretical value, i.e., 5. The NRSME of the CATF based amplitude spectrum reconstruction is 2.14% for $y = 5x^2$, and 2.22% for $y = 5x^3$.

Fig. 3 shows the simulation results for the Hammerstein and Wiener systems. In the Hammerstein system, the first block generates the harmonic and intermodulation responses from the second-order power function. After the band-pass filtering of the second block, the responses outside the band-pass range decrease. Both the nonlinear behavior of power function and the dynamic behavior of the filter are reflected in the CATF,

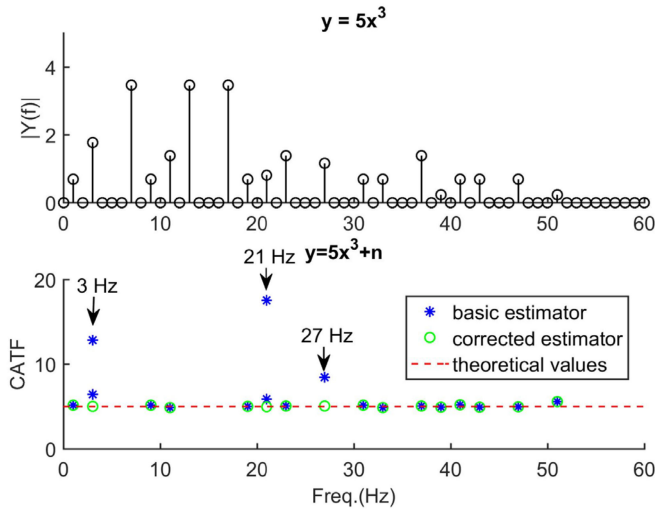


Fig. 4. Amplitude spectra and comparison of basic vs. corrected estimator of CATF for the third order power function with the multisine stimulus of 7, 13 and 17 Hz. The overlapping response frequencies are at 3, 21 and 27 Hz.

where the CATF values are present at the second-order harmonic and intermodulation frequencies and reduce at the frequencies outside the band-pass range, showing the shape of the filter. The NRSME of CATF based amplitude spectra reconstruction is 4.11% for Hammerstein system. In the Wiener system, the first block generates the linear responses from the filter, showing decreased amplitudes for frequency components at 7 and 29 Hz. Due to this dynamic effect, the harmonic and intermodulation responses originated from the stimulus components at 7 and 29 Hz reduce compared to the static power function. This dynamic nonlinear behavior is reflected in the CATF. Only the CATF value at the harmonic (26 Hz) of 13 Hz maintains the same value as the static power function (which is equal to 5 for $y = 5x^2$) while the others decrease. The NRSME of CATF based amplitude spectra reconstruction is 6.24% for Wiener system, which is larger than the Hammerstein system and the static power function with the same order of nonlinearity.

When the combinations of stimulation frequencies have overlaps in response frequencies, the basic CATF computed by Eq. (3) has a large error. In this case, we need to use Eq. (7) to get the corrected CATF. The comparison between the basic and the corrected estimators is provided in Fig. 4. CATF values estimated by Eq. (3) are far away from the theoretical value in the overlapping frequencies, i.e., 3, 21 and 27 Hz, with a much larger NRSME (NRSME 26.79%) compared to the corrected estimator (NRSME 2.86%). The CATF values obtained by the corrected estimator (Eq. (7)) are around the theoretical value with a very small NRSME (2.86%).

B. Application to the Human Proprioceptive System

A periodic somatosensory stimulation evokes a steady-state response in the cortex, which is phase-locked to the stimulus [2], [27]. Fig. 5 shows a topographic map of the signal power field of EEG responses to the perturbation, showing localized

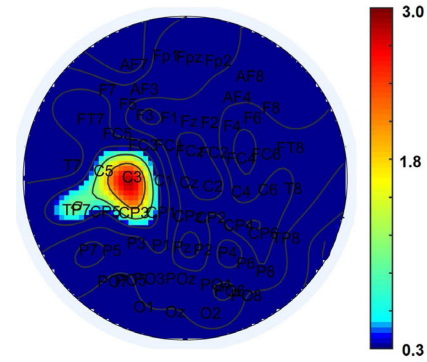


Fig. 5. Topographic map of the power field of EEG responses to the perturbation for a typical subject. Electrode labels are provided for those in 10–20 system. The peak value is found at the electrode C3.

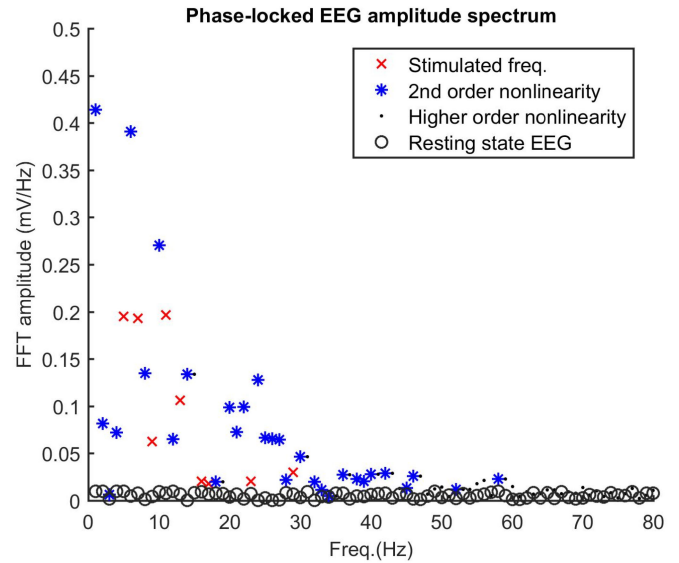


Fig. 6. Amplitude spectrum of phase-locked EEG for a typical subject at different frequencies, as compared to the amplitude spectrum resting-state EEG recorded from the same subject when there is no wrist perturbation provided to the subject.

activity with the peak value at C3. Fig. 6. shows the amplitude spectrum of phase-locked EEG component at C3 for a typical subject. We compute the power spectrum ratio of second-order nonlinearity over the whole spectrum. We found that 76% of signal power is in the second-order nonlinearity. This result confirms the dominance of second-order nonlinearity in the EEG response to perturbation. Fig. 7. show the mean and standard deviation of normalized CATF over all subjects at the second-order nonlinearity. The large CATF values are shown in the low-frequency range (<25 Hz) with the peak around 10 Hz. The CATF amplitude decays with higher frequencies indicating the presence of filter dynamics in the nervous system. However, the CATF spectrum does not show a smooth filter shape, as seen with the Hammerstein system in the simulations. Therefore, the response cannot be generated from a Hammerstein structure alone (compared to the simulation result in Fig. 3.). This result

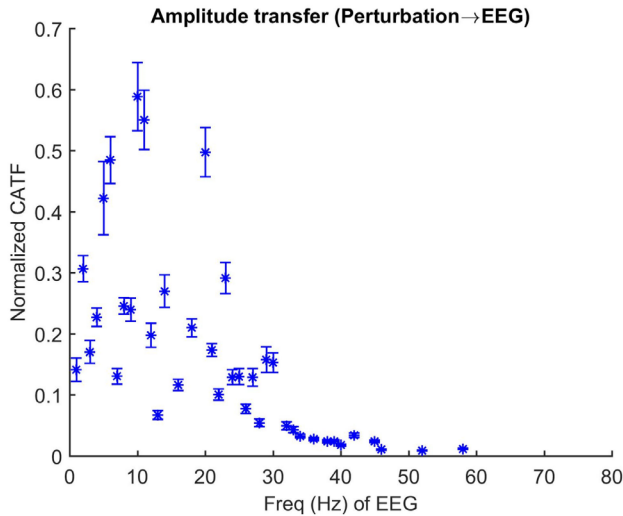


Fig. 7. Mean and standard deviation of normalized CATF over all subjects at the second-order nonlinearity.

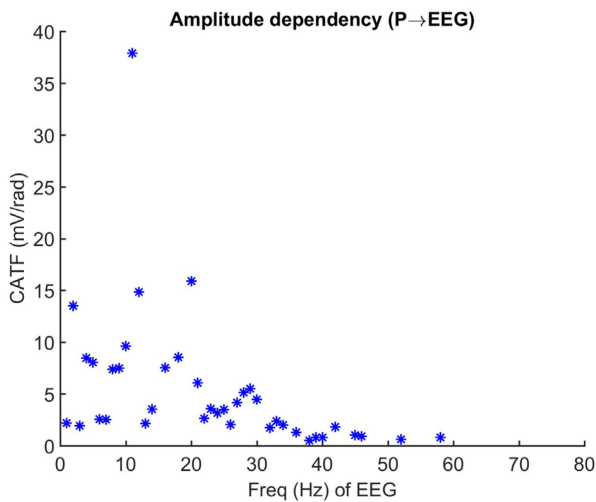


Fig. 8. Non-normalized values of the obtained CATF for a typical subject.

is consistent over subjects (indicated by the small variances in Fig. 7). Fig. 8 presents the non-normalized CATF for a typical subject).

IV. DISCUSSION

Cross-frequency amplitude transfer function is developed based on the general nonlinear frequency mapping rule (see Eq. (1)) [14] to assess the nonlinear amplitude transfer in the nervous system. Different from generalized phase synchrony and coherence measures [10], [14], the CATF is a measure assessing nonlinear phase-locked interactions between the stimulus and the response from the signal amplitude.

Demonstrated in model simulations, the CATF can be used to assess different order interactions in a static nonlinear system, as well as systems containing dynamics described by Hammerstein and Wiener systems. Simulation results show that the CATF can well estimate the amplitude transfer (nonlinear gain) across

different frequencies in a nonlinear system for different nonlinear orders. Better performance is achieved for static nonlinear systems compared to dynamic systems, where the result for the Hammerstein system is better than that for the Wiener system. For dynamic systems, filter dynamics can decrease the response signal power and lead to poor SNR at the filtered frequencies. Thus, the performance of CATF on dynamic systems is not as good as static systems. In the Wiener system, the filter dynamic is before the static nonlinear element, so the signal power has reduced before entering the nonlinear part, which leads to low SNR in more frequencies in comparison with Hammerstein system. Users can improve the CATF estimation either by increasing the power of stimulus signal or by performing the experiments with more trials. When the combinations of stimulation frequencies are overlapping in response frequencies, the estimator of CATF is corrected (by Eq. (7)) to reduce the estimation error.

Previous studies have reported the nonlinear behavior of the human proprioceptive system, showing harmonic and intermodulation responses to the mechanical multisine perturbation based on the power spectrum of EEG and phase coupling between the stimulus and the response [3], [10], [13], [14]. A recent study demonstrated that more than 80% of the signal power in the EEG response occurs at the non-stimulated frequencies, which indicates that the human proprioceptive system is highly nonlinear [3]. Here, we applied CATF to investigate the nonlinear amplitude transfer in the human proprioceptive system; and the phase transfer and time delay in such a system have been revealed in our previous studies [10], [23].

The amplitude spectrum of phase-locked EEG component shows the dominance of second nonlinearity in the EEG response to the mechanical perturbation, which is in line with previous studies [14], [23], [24]. Moreover, the second-order interaction such as intermodulation between two stimulation frequencies is thought to be associated with the mechanism of neuronal integration of sensory information in the nervous system [28]. Thus, we focused on the second-order nonlinearity.

In the somatosensory pathway, the proprioceptive information is encoded by mechanoreceptors (i.e., muscle spindles), transmitted through synapses in the dorsal column nuclei, and reaches the somatosensory cortex via the thalamocortical somatosensory radiation. Previous studies have reported the second-order nonlinearity in the sensorimotor system which could be partially explained by the nonlinear behavior of muscle spindles using a Hammerstein structure [24]. However, these studies mainly focus on the muscular response to the proprioceptive stimulus at the spinal level. Recent studies demonstrated rich nonlinearity and complicated dynamics of thalamocortical radiation [2], [29], which is also a part of the somatosensory afferent pathway in the proprioceptive system.

The shape of CATF spectrum suggested that complicated dynamics in the cortical response to the proprioceptive stimulus. These dynamics may not only be resulted from the velocity filter in the muscle spindle [24] but also from the dynamic interaction in thalamocortical radiation. Especially, our results show a large amplitude transfer in the alpha band (~ 10 Hz). The alpha band activity of EEG is known to be originated from the thalamocortical network [30].

V. CONCLUSION

This paper proposes a novel measure to assess the nonlinear amplitude transfer in the nervous system. The CATF can be applied to both static nonlinearities and dynamic nonlinear systems described by Hammerstein and Wiener structures. The application of CATF quantifies the nonlinear amplitude transfer from the stimulus to the cortical response in the human proprioceptive system. As a useful complement to our previous findings based on phase transfer and nonlinear coherence [10], [14], our results could lead to a better understanding and quantitative modeling of the human proprioceptive system. The proposed approach has the potential to explore nonlinear interactions in the sensorimotor system and to contribute to motor control and rehabilitation studies.

ACKNOWLEDGMENT

The authors would like to thank L. Eleftheriou for collecting the experimental dataset. The authors would like to thank all members of 4D-EEG consortium at the Delft University of Technology, Northwestern University, and VU University Amsterdam Medical Center for useful discussions.

REFERENCES

- [1] G. R. Müller-Putz *et al.*, "Steady-state visual evoked potential (SSVEP)-based communication: Impact of harmonic frequency components," *J. Neural Eng.*, vol. 2, no. 4, p. 123, Oct. 2005. [Online]. Available: <https://iopscience.iop.org/article/10.1088/1741-2560/2/4/008>
- [2] A. J. Langdon, T. W. Boonstra, and M. Breakspear, "Multi-frequency phase locking in human Somatosensory cortex," *Prog. Biophys. Mol. Biol.*, vol. 105, no. 1, pp. 58–66, Mar. 2011.
- [3] M. P. Vlaar *et al.*, "Quantifying nonlinear contributions to cortical responses evoked by continuous wrist manipulation," *IEEE Trans. Neural Syst. Rehabil. Eng.*, vol. 25, no. 5, pp. 481–491, May 2016.
- [4] T. D. Sanger *et al.*, "Nonlinear sensory cortex response to simultaneous tactile stimuli in writer's cramp," *Mov. Disord.*, vol. 17, no. 1, pp. 105–111, Jan. 2002.
- [5] Y. Yang *et al.*, "Nonlinear coupling between Cortical oscillations and muscle activity during isotonic wrist flexion," *Front. Comput. Neurosci.*, vol. 10, p. 126, Dec. 2016. [Online]. Available: <https://www.frontiersin.org/articles/10.3389/fncom.2016.00126/full>.
- [6] Y. Yang *et al.*, "Unveiling neural coupling within the Sensorimotor system: Directionality and nonlinearity," *Eur. J. Neurosci.*, vol. 48, no. 7, pp. 2407–2415, Oct. 2018.
- [7] F. L. da Silva, J. P. Pijn, and P. Boeijinga, "Interdependence of EEG signals: Linear vs. nonlinear associations and the significance of time delays and phase shifts," *Brain Topogr.*, vol. 2, no. 1–2, pp. 9–18, Sep. 1989.
- [8] J. Shils, M. Litt, B. Skolnick, and M. Stecker, "Bispectral analysis of visual interactions in humans," *Electroencephalogr. Clin. Neurophysiol.*, vol. 98, no. 2, pp. 113–125, Feb. 1996.
- [9] J. C. Sigl and N. G. Chamoun, "An introduction to bispectral analysis for the Electroencephalogram," *J. Clin. Monit.*, vol. 10, no. 6, pp. 392–404, Nov. 1994.
- [10] Y. Yang *et al.*, "A general approach for quantifying nonlinear connectivity in the nervous system based on phase coupling," *Int. J. Neural Syst.*, vol. 26, no. 1, p. 1550031, Feb. 2016. [Online]. Available: <https://www.worldscientific.com/doi/abs/10.1142/S0129065715500318>
- [11] P. Tass *et al.*, "Detection of n: M phase locking from noisy data: Application to magnetoencephalography," *Phys. Rev. Lett.*, vol. 81, no. 15, p. 3291, Oct. 1998.
- [12] F. He *et al.*, "Nonlinear interactions in the Thalamocortical loop in essential tremor: A model-based frequency domain analysis," *Neuroscience*, vol. 324, pp. 377–389, Jun. 2016.
- [13] Y. Yang *et al.*, "Probing the nonlinearity in neural systems using cross-frequency coherence framework," *IFAC-PapersOnLine*, vol. 48, no. 28, pp. 1386–1390, 2015. [Online]. Available: <https://www.sciencedirect.com/science/article/pii/S240589631502950X>
- [14] Y. Yang *et al.*, "A generalized coherence framework for detecting and characterizing nonlinear interactions in the nervous system," *IEEE Trans. Biomed. Eng.*, vol. 63, no. 12, pp. 2629–2637, Dec. 2016.
- [15] J. Victor and R. Shapley, "A method of nonlinear analysis in the frequency domain," *Biophys. J.*, vol. 29, no. 3, p. 459, Mar. 1980.
- [16] S. A. Billings, *Nonlinear System Identification: NARMAX Methods in the Time, Frequency, and Spatio-Temporal Domains*. West Sussex, UK: John Wiley & Sons, 2013, pp. 1–14.
- [17] R. Tian *et al.*, "A novel approach for modeling neural responses to joint perturbations using the NARMAX method and a hierarchical neural network," *Front. Comput. Neurosci.*, vol. 12, p. 96, Dec. 2018. [Online]. Available: <https://www.frontiersin.org/articles/10.3389/fncom.2018.00096/full>
- [18] S. E. Eikenberry and V. Z. Marmarelis, "A nonlinear autoregressive Volterra model of the Hodgkin–Huxley equations," *J. Comput. Neurosci.*, vol. 34, no. 1, pp. 163–183, Feb. 2013.
- [19] N. Sinha *et al.*, "Cross-frequency coupling in descending motor pathways: Theory and simulation," *Front. Syst. Neurosci.*, vol. 14, Jan. 2020. [Online]. Available: <https://www.frontiersin.org/articles/10.3389/fnsys.2019.00086/abstract>
- [20] J. D. Victor, "Nonlinear systems analysis: Comparison of white noise and sum of sinusoids in a biological system," *Proc. Natl. Acad. Sci. USA*, vol. 76, no. 2, pp. 996–998, Feb. 1979.
- [21] K. J. Friston, "Brain function, nonlinear coupling, and neuronal transients," *Neuroscientist*, vol. 7, no. 5, pp. 406–418, Oct. 2001.
- [22] A. Nieder and E. K. Miller, "Coding of cognitive magnitude: Compressed scaling of numerical information in the primate prefrontal cortex," *Neuron*, vol. 37, no. 1, pp. 149–157, Jan. 2003.
- [23] Y. Yang *et al.*, "Nonlinear connectivity in the human stretch reflex assessed by cross-frequency phase coupling," *Int. J. Neural Syst.*, vol. 26, no. 8, p. 1650043, Dec. 2016. [Online]. Available: <https://www.worldscientific.com/doi/abs/10.1142/S012906571650043X>
- [24] R. E. Kearney and I. W. Hunter, "Nonlinear identification of stretch reflex dynamics," *Ann Biomed Eng.*, vol. 16, no. 1, pp. 79–94, Jan. 1988.
- [25] S. F. Campfens *et al.*, "Quantifying connectivity via efferent and afferent pathways in motor control using coherence measures and joint position perturbations," *Exp. Brain Res.*, vol. 228, no. 2, pp. 141–153, Jul. 2013.
- [26] S. Hagihira *et al.*, "Practical issues in bispectral analysis of Electroencephalographic signals," *Anesth Analg.*, vol. 93, no. 4, pp. 966–970, Oct. 2001.
- [27] S. Tobimatsu, Y. M. Zhang, and M. Kato, "Steady-state vibration somatosensory evoked potentials: Physiological characteristics and tuning function," *Clin. Neurophysiol.*, vol. 110, no. 11, pp. 1953–1958, Nov. 1999.
- [28] C. Gundlach and M. M. Müller, "Perception of illusory contours forms intermodulation responses of steady state visual evoked potentials as a neural signature of spatial integration," *Biol Psychol.*, vol. 94, no. 1, pp. 55–60, Sep. 2013.
- [29] J. Roberts and P. Robinson, "Quantitative theory of driven nonlinear brain dynamics," *Neuroimage*, vol. 62, no. 3, pp. 1947–1955, Sep. 2012.
- [30] F. L. da Silva, "Neural mechanisms underlying brain waves: From neural membranes to networks," *Electroencephalogr. Clin. Neurophysiol.*, vol. 79, no. 2, pp. 81–93, Aug. 1991.